On the Number of Cosmic Strings in Dark Energy Cosmologies

R. Consiglio · O. Sazhina · G. Longo · M. Sazhin · F. Pezzella

Abstract The number of cosmic strings in the observable universe is relevant in determining the probability to detect the presence of cosmic strings through their gravitational signatures. In particular, we refer to the observation of gravitational lensing events and anisotropy in the CMB radiation induced by cosmic strings. In this paper, a simple method is adopted to obtain an approximate estimate of the number of segments of cosmic strings, crossing the particle horizon, which fall inside the visible (i. e. observed) part of the universe. We show that a different choice of the CDM cosmological model, which affects volumes, does actually have only a small weight on the expected number of cosmic string segments. Of this number, the fraction realistically detectable may be significantly smaller.

1 Introduction

Cosmic strings are line-like topological defects which may have formed during a symmetry breaking phase transition in the early universe. The existence of topological defects in spacetime was first theorized by Kibble in 1976 [1]. Formation

R. Consiglio
Dipartimento di Scienze Fisiche, Università Federico II, via Cintia 6, 80126 Napoli, Italy
E-mail: dmsqco@libero.it

O. Sazhina
Sternberg Astronomical Institute, M.V. Lomonosov Moscow State University, University pr. 13, Moscow, Russia

G. Longo
Dipartimento di Scienze Fisiche, Università Federico II, via Cintia 6, 80126 Napoli, Italy
Visiting associate, Department of Astronomy, California Institute of Technology, Pasadena, 90125 CA, USA

M. Sazhin
Sternberg Astronomical Institute, M.V. Lomonosov Moscow State University, University pr. 13, Moscow, Russia

F. Pezzella
INFN - Sezione di Napoli, Università Federico II, via Cintia 6, 80126 Napoli, Italy

and evolution of cosmic defects were extensively studied in the subsequent decades [2,3,4,5] for their cosmological implications. Due to the compatibility of their existence with cosmological observations and their topological stability, a special interest has always been focused on cosmic strings [6,7,8]. This class of linear defects is a generic prediction in quantum field theory and grand unified theories (GUTs) as well as in string and M-theories. The predicted cosmic strings are extremely thin but very massive objects, characterized by a huge energy and interactions essentially of gravitational nature, whose intensity is measured by the dimensionless tension parameter $G\mu/c^2$. The value of this quantity is model dependent; for a string produced at a GUT transition $G\mu/c^2$ is of order 10^{-6} or 10^{-7}. Although observations rule out the idea of topological defects as an alternative theory to inflation, the coexistence between cosmological inflation and cosmic strings is apparent in those inflationary scenarios which can themselves give rise to strings in a phase transition which occurs at the last stages of inflation. This is the case of hybrid inflation models in standard cosmology as well as brane/antibrane inflation models in string cosmology which are of hybrid inflation type. In this framework, a composite family of stable strings may exist in certain classes of models of warped compactifications or large compact extra dimensions which yield string tensions decoupled from Planck scale in the range $10^{-12} \leq G\mu/c^2 \leq 10^{-6}$ and hence compatible with observational limits [9,10,11]. Differently from solitonic strings, cosmic superstrings can exist as F and D strings leading to more complicated FD-networks involving the formation of junctions between strings of different tensions [12,13]. Although they can have different properties related to the different context in which they arise, cosmic superstring are expected to share with the ordinary solitonic strings the same scale-invariance property of the characteristic length scales of the network that they can form. Since their energy density may influence the dynamics of the universe, consistency with present day observations imposes constraints on the number density of cosmic strings. To date, cosmic (super)strings are still theoretical objects, nevertheless theoretical advances together with upcoming observational data might provide stronger constraints on their characteristic parameters and make their eventual detection a test of generic predictions of standard or alternative theories. Observations of such strings would provide direct information on fundamental physics and evolution of our universe and maybe the first experimental evidence of a string theory cosmological model underlying the structure of spacetime.

Cosmic (super)strings may have a number of cosmological effects. The most interesting observational signatures stem from their gravitational interactions. While specific signatures are expected in models where strings couple to other forces, gravitational effects are common to all cosmic (super)strings and are controlled by the dimensionless tension parameter. A special class of gravitational effects originates from the string peculiar way to deform the spacetime around it. The spacetime around a cosmic string is conical, namely, it is flat everywhere except for a missing wedge where points on the opposite edges are identified.Thus, spacetime looks like a cone with a singularity located at the apex of the cone. Any circular path at constant distance from the apex around the string is less than a circumference by the deficit angle $\Delta = 8\pi G\mu/c^2$. This geometry leads to observable effects, such as the Kaiser-Stebbins effect (KS) [14] and gravitational lensing. The former appears as line discontinuities in the CMB temperature caused by a segment of cosmic string moving between the observer and the cosmological pho-

tosphere as photons passing by the string move perpendicularly to the plane that contains the string segment. Photons from the last scattering surface streaming by either side of the string will be observed with a redshift or blueshift (ahead of or behind the moving string respectively) proportional to the string tension and the string velocity transverse to the line of sight. Gravitational lensing by a long cosmic string occurs as light from a distant source beyond the string may reach the observer by two different paths around either side of the string thus producing a double image of the source with angular separation proportional to the conical deficit angle $8\pi G\mu/c^2$.

The observational signatures of cosmic strings depend on the characteristic parameters and on the details of the evolution of the string network which in turn depend on what happens when two strings intersect. A fundamental feature which differentiates a network of cosmic superstrings from a network of ordinary field-theory cosmic strings is their reduced intercommutation probability P which determines the evolution of a string network towards scaling regime. For FD-networks, P can be significantly less than unity, depending on the type of strings and compactification and on the string coupling constant g_s. As a consequence of the smaller intercommutation probabilities associated with strings of different tensions, in a cosmic superstrings network each type of string may have a different number density. This means that the same fraction of CMB anisotropy can be sourced either by many light strings or by a few heavy ones but it also means that the total amount of strings in the network must be increased by some factor related to the intercommutation probabilities, which implies stronger constraints on tensions. The eventual presence of Y-shaped junctions of two strings joined by a third after intercommutation processes could be detected by cosmic string gravitational lensing or by observation of the KS effect. In the latter case, a different temperature in each of the three patches of sky is expected to be observed, while in the former case the relativistic motion of the binding strings could also lead to an enhancement of the cosmic string lensing angle by some factor which would be moderate for a typical network motion [15, 16, 17, 18].

In the present paper we consider the case of classical cosmic strings for which the string tension is directly related to the energy scale of the symmetry breaking and the intercommutation probability is essentially $P = 1$. In fact, even though ultrarelativistic Abelian Higgs strings can pass through each other due to a double intercommutation with the net result that no ends are exchanged [19], the typical velocities found in simulations for scaling networks of cosmic strings are below the ultrarelativistic threshold, so that the assumption $P = 1$ generally holds. On the other hand, the rms velocities comparable to the speed of light found in numerical simulations [20, 21, 22, 23, 24, 25, 26] are sufficiently high as to guarantee the detectability of their signature in the CMB radiation, if such strings do exist. The number of cosmic strings contained in the volume of the observable universe is also a relevant parameter to determine the probability of observing cosmic strings in gravitational lensing events as well as the density of step-like temperature discontinuities related to the KS effect [27, 28, 29]. In Section 2 we describe a simple method to obtain an approximate estimate of the number of segments of cosmic strings crossing the observable universe. In particular, for their observational relevance, we consider the volume inside the last scattering surface and inside the sphere of optical sources respectively for KS effect and gravitational lensing observations. We extend the previous approach to string networks embedded in cosmological back-

grounds, variants of the ΛCDM, where the constant parameter Λ is replaced with a dynamical scalar field. For a comparison of results, we consider, for simplicity, spatially flat cosmological models where the cosmic fluid is a mixture of matter and quintessence or a phantom constituent (a time varying component of the energy density of the universe with negative or super-negative pressure, $p < -\rho$) characterized by the ratio of pressure to energy density in the range $-1 \leq w < 0$ and $w < -1$, respectively, whereas $w = -1$ coincides with the cosmological constant case. In the above intervals we choose in particular $-1 \leq w \leq -0.5$ and $w = -1.5$ respectively for the quintessence and phantom components as they are compatible with constraints from large scale structure and CMB observations combined with SNe Ia data. In Section 3 we outline some features connected with numerical simulations and their underlying models in relation to the scaling property of the string network upon which relies the estimate of the number of string segments. We discuss our results with particular reference to the range of redshifts in the visible universe where the calculation of the number of string segments can be trusted, taking into account the informations about the scaling regimes provided by numerical simulations.

Without a loss of generality, in what follows we shall use the cosmological parameters of the ΛCDM concordance model, which fit the majority of observations [30,31]:

$$\Omega_m \simeq 0.27 \qquad \Omega_\Lambda \simeq 0.73 \qquad H_0 \simeq 71 km/s/Mpc. \tag{1}$$

2 Number of segments of cosmic string crossing the observable universe

2.1 Cosmic string networks in a ΛCDM universe

An approximate estimate of the number of string segments crossing a given volume of the observable universe can be obtained taking into account that Kibble's one-scale model can be conveniently used to study large-scale properties. The single scale L, which can be identified with the persistence length or the mean inter-string distance, is defined as the length such that any volume L^3 will contain on average a string segment of length L. By causality, L is bounded by the size of the particle horizon, d_{PH}:

$$L = A_i \; d_{PH} \tag{2}$$

where:

$$0 < A_i \leq 1 \qquad i = r, m \tag{3}$$

with $r \equiv radiation$ and $m \equiv matter$. The quantity:

$$A_i^{-1} = \frac{d_{PH}}{L} \tag{4}$$

expresses the scaling property: in the radiation-dominated era (after the transient friction-dominated period) and in matter-dominated era (after the radiation-matter transitional period) the network approaches a scaling regime in which L

remains a constant fraction of the particle horizon, as well as the energy in the form of strings remains a constant fraction of the total energy of the universe. Therefore, the above quantity is the result of the efficiency of the various energy-loss processes that a network of strings undergoes. This provides us with an elementary cell, containing a single string segment, whose volume can be calculated being known A_i, from numerical simulations, and the particle horizon distance d_{PH}:

$$d_{PH} = \frac{c}{H_0} \int_0^\infty \frac{dz}{E(z)} \tag{5}$$

where:

$$E(z) = \left[\sum_{i \in I} \Omega_i (1+z)^{3(w_i+1)} \right]^{1/2} \qquad I = \{\Lambda, k, m, r\} \tag{6}$$

where w_i is the equation-of-state parameter for the ith fluid. Let us define the distance traveled by a photon from the emission point, at a time $t = t_*$, to an observer at present time t_0:

$$d(z_*) = \frac{c}{H_0} \int_0^{z_*} \frac{dz}{E(z)}. \tag{7}$$

In particular, we are concerned with the volume contained in the spherical surface, named *last scattering surface* (LSS), given by the set of points in space at a distance such that photons emitted at decoupling time reach present-day observers. Then at any time $t_* \leq t_{LSS}$, belonging to the matter-dominated era, the distance to any point inside the LSS can be written as:

$$d(z_*) = \frac{c}{H_0} \int_0^{z_*} \frac{dz}{\sqrt{\Omega_m (1+z)^3 + \Omega_\Lambda}}. \tag{8}$$

With our choice of the concordance-model cosmological parameters (1), $\Omega_R \simeq 8.4 \times 10^{-5}$ (where Ω_R includes the photon density Ω_r and the neutrino density Ω_ν) and $\Omega_k \simeq -0.011$ [30,31] we have:

$$d_{PH} = \frac{c}{H_0} \int_0^\infty \frac{dz}{E(z)} \simeq \frac{c}{H_0} \, 3.4 \tag{9}$$

which does not differ significantly (less than one percent, $\sim 0.98\%$) from the value we obtain by taking only Ω_m and Ω_Λ.

The distance $d(z)$ can be conveniently expressed in terms of the particle horizon distance by means of a proportionality factor incorporating the dependence on z:

$$d(z) = B(z) \, d_{PH} \qquad , \qquad 0 < B(z) < 1. \tag{10}$$

Let us now consider a cube with side equal to the diameter of the spherical volume centered on the present time observer, $2d(z)$, with:

$$z_0 < z \leq z_{LSS} \tag{11}$$

where $z_0 = 0$ is the redshift at present time and $z_{LSS} = 1100$ is the redshift corresponding to the last scattering time. The largest cube, for $z = z_{LSS}$, circumscribes the CMB sphere so that all strings that enter the particle horizon and may have

potentially observable effects on the CMB radiation are inside this volume. For any given value of the redshift in the interval (11), the number of string segments crossing the volume of the corresponding cube can be then computed as:

$$N(z) = \frac{[2\,d(z)]^3}{L^3} = \frac{8\,B^3(z)\,d_{PH}^3}{A_m^3\,d_{PH}^3} = \frac{8\,B^3(z)}{A_m^3}. \tag{12}$$

Similarly in the radiation-dominated era $N(z)$ can be obtained by substituting in the above eq. (12) A_m with A_r and the definition (7) for the distance.

$$N(z) = \frac{8\,B^3(z)}{A_r^3}. \tag{13}$$

2.2 Dark energy cosmological models

In the previous section we chose for definiteness a particular FRW cosmology, the ΛCDM model, as the cosmological background for the evolving string network. In the present section we generalize to a broader class of models by replacing the static homogeneous energy component, with positive energy density and negative pressure Λ, with a dynamical, time-dependent and spatially inhomogeneous energy component, named *dark energy*, whose negative pressure drives the accelerated expansion of the universe currently observed. In particular, the class of cosmological models we consider are spatially flat FRW space-times dominated by dark energy at late times, after radiation (photons and relativistic neutrinos) and matter (ordinary and cold dark matter) dominance.

The spacetime, for a spatially-flat expanding universe, is described by the metric [32]:

$$ds^2 = c^2 dt^2 - a^2(t)d\mathbf{x}^2. \tag{14}$$

Defining the conformal time η by:

$$d\eta = \frac{cdt}{a(t)} \tag{15}$$

the metric can be conveniently expressed in terms of η as:

$$ds^2 = a^2(\eta)\left(d\eta^2 - d\mathbf{x}^2\right). \tag{16}$$

The scale factor $a(\eta)$ is determined from the Friedmann equation, which can be written in the form:

$$\left(\frac{da(\eta)}{a^2(\eta)d\eta}\right)^2 = H_0^2\left[\Omega_m\left(\frac{1}{a(\eta)}\right)^3 + \Omega_{de}\left(\frac{1}{a(\eta)}\right)^{3(1+w)}\right] \tag{17}$$

where Ω_{de} is the dark energy density parameter, related to the current contribution of about 73% to the total energy density of the universe, whose budget should also contain the contribution of radiation (as well as spatial curvature), which we have neglected being less than one percent. w is the ratio of pressure to energy density which defines the equation of state for dark energy:

$$p_{de} = w\rho_{de}c^2. \tag{18}$$

Current cosmological observations restrict the values of the equation-of-state parameter in the interval:

$$w \in [-1.5, -0.5]. \tag{19}$$

Scalar field models can yield a time-varying equation-of-state parameter such that at large redshifts w corresponds to quintessence ($w > -1$), while in later stages, at low redshifts, w becomes much more negative denoting a phantom energy component ($w < -1$). In the very late universe, the phantom energy density ($\rho_p > 0$) can grow allowing the parameter w to reach an observationally compatible value slightly below minus one [33, 34, 35].

Let's now derive in this context the expression of the distance traveled by a photon emitted at $t = t_e$ and the particle horizon distance for an observer at present time t_0. Using the conformal gauge, photons traveling on radial null geodesics, given by $ds^2 = 0$, move unit comoving distance per unit conformal time $d\eta = \pm dx$. Thus, in the metric conformally flat the light cones are Minkowskian and the speed of light is one. Hence, in conformal coordinates, light emitted at conformal time η_e will be observed at conformal time η_o at comoving distance:

$$D(z_e) = \eta_o - \eta_e. \tag{20}$$

Then for a present-time observer $\eta_o \equiv \eta_0$ and the distance to the emitting source can be obtained from the first Friedmann equation:

$$H_0(\eta_0 - \eta_e) = \int_{a_e}^{1} \frac{da}{\sqrt{a}\sqrt{\Omega_m + \frac{\Omega_{de}}{a^{3w}}}}. \tag{21}$$

From the scale factor-redshift relation, $a = (1 + z)^{-1}$, with $a(t_0) \equiv a_0 = 1$, we obtain the distance to an object with redshift z_e:

$$D(z_e) = \frac{c}{H_0} \int_{0}^{z_e} \frac{dz}{(1 + z)^{3/2}\sqrt{\Omega_m + \Omega_{de}(1 + z)^{3w}}} \tag{22}$$

and by letting $z_e \to \infty$ (i. e. $t_e, a_e \to 0$) we obtain the distance to the particle horizon, which for the parameter w in the above interval (19) has the following solution [36]:

$$D_{PH} = \frac{2c}{\sqrt{\Omega_m}H_0} F\left(\frac{1}{6|w|}, \frac{1}{2}; \frac{6|w| + 1}{6|w|}; -\frac{\Omega_{de}}{\Omega_m}\right) \tag{23}$$

where $F(a, b; c; z)$ is the Gauss hypergeometric function.

Recalling eq. (10), since the number of cosmic string segments in a given volume around the observer at $t = t_0$ is proportional to $B^3(z)$, we show in Fig. 1 for different values of w the behavior of $B(z)$, which in the general cosmological setting with dark energy is:

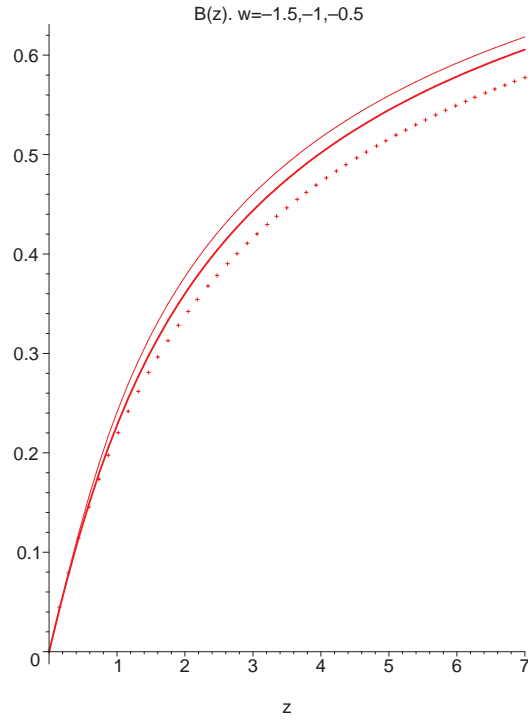$$B(z) = \frac{D(z)}{D_{PH}}. \tag{24}$$

Fig. 1 $B(z)$ plotted for the equation-of-state parameter varying inside the interval $w \in [-1.5, -0.5]$, for z in the optical-source range. The light curve corresponds to $w = -0.5$, solid curve corresponds to $w = -1$, while diamonds correspond to $w = -1.5$.

3 Discussion and results

The number of string segments $N(z)$ has been determined in the range of redshifts of interest for observations by using the constant quantity A_m associated with the scaling law, thus assuming that the network has already reached the scaling regime in the matter-dominated era by the time t_{LSS} which is the upper limit of the range of redshifts (11). As a matter of fact there is a transition period between the radiation-dominated and matter-dominated eras where the string network will

be far from the type of equilibrium that characterizes a scaling solution for a time dependent on how fast is the network's response to the change in expansion rate. Thus, the range of redshifts in the matter-dominated era within which we can trust a "string counting" based on the scaling property could be well below z_{LSS} and then below the range of radio surveys for searching of cosmic string signatures in the CMB radiation. A similar limit, this time at very small redshifts, namely $z \approx 0.5$, is also to be taken into account since there is a further transition between the matter-dominated era and the dark-energy-dominated era [37,38]. The effect of this transition to a cosmological era where the universe expands exponentially will be a reduction of the string velocity, which prevents reconnection, affecting the scaling behavior and, at the same time, a dilution which might lead to a small number density of the leftover network [39,40].

The scaling property, which implies it makes sense to consider the possibility of the string existence in our universe and search for their observable effects, is the first fundamental information about a network of cosmic strings yielded by numerical simulations. These are essentially based on the field theory Abelian Higgs (AH) model and the Nambu-Goto (NG) model. The latter one relies on the assumption that as the scale of the string diameter is much smaller than any cosmological scale, such strings can be studied in the zero width approximation.

In particular, in NG simulations the time required for the long string component relaxation to the scaling regime in the matter-dominated era can appear decidedly longer than the transient taken to reach scaling in the radiation-dominated era so that the transition period might last far beyond the end of the decoupling time. Some difference can be found in the NG simulations results related to a different choice of the long component of the network, which can include all loops but those evolving on non-intersecting trajectories (stable loops that cannot rejoin the network) [26] or only super-horizon loops. In the latter case the long string component could reach the scaling regime in a relatively short time showing little time delay between the change in the expansion law and the response of the network. However, for what it concerns the loop component, its energy density also reaches a scaling evolution but the loop distribution takes more time to reach the scaling regime and the transition period is longer for the smaller loops [20,23].

In AH simulations the effects of matter-radiation transition are not apparent in the network evolution. The first simulations yield approximately even the same value $A_r \simeq A_m \approx 0.3$ [24], although this result is admittedly a consequence of a simulation size about the minimum required to study a scaling network of strings and recent improved simulations performed by the same authors yield a different result for the scaling parameters in matter- and radiation-dominated era, with $A_r \simeq 0.26$ and $A_m \simeq 0.29$ [41].

The reason for differences between simulation results lies mainly in the model at the basis of the simulations. The AH model includes the small-scale physics near the string width, which has a significant role in the string dynamics. While in AH simulations energy from the strings is converted into massive gauge and Higgs radiation, in NG simulations this decay channel is not available and the string length density is significantly higher, with the long strings first converted into small loops and subsequently decaying via gravitational radiation. This additional decay channel in the field theoretic simulations by direct massive radiation is the primary energy-loss mechanism for long strings and causes AH strings to scale without gravitational radiation. In the NG scenario, particles are produced

only near cusps, which determines much weaker constraints on the production of extremely energetic Standard Model particles (the Ultra-High Energy Cosmic Rays) than in the AH model. On the other hand, in the AH model there are no constraints from gravitational radiation whereas in the NG case the strongest limits come from millisecond pulsar timing which depend sensitively on details of the loop distribution and dynamics. The number of loops in the simulation volume is substantially less in field theory simulations than in NG where a population of non-intersecting loops remaining stable is found while in AH, where massive radiation is available, loops radiate and shrink. As regards the relevant component for CMB: the long (super-horizon) strings, the results yielded by the two types of simulations are quite different in most respects, such as the inter-string separation and therefore the string density which results significantly lower in AH than in NG simulations. Similarly, the rms velocities probably due to backreaction from the massive radiation are lower in AH than in NG simulations. In fact, AH simulations give $\approx 0.5c$ [8] in both the radiation and matter eras whereas NG simulations give distinct values in the two cosmological eras both generally above $0.6c$.

A specific problem related to field theory simulations is that computational constraints require the string width to be artificially increased in order to keep it above the simulation resolution. Although this does not significantly affect the CMB power spectra results a much relevant problem associated with the string width is that the 3D boxes required imply a reduction of the dynamical range. The fact that in AH simulations most of the network energy is emitted through field radiation, until the point that loop production is almost absent, has been supposed to be a consequence of a low resolution in AH simulation compared to NG ones. On the other hand, the accuracy of the NG simulations with regard to small-scale structure and loop production has also been questioned. In fact, the NG approximation fails close to the string width, that is, at cusps and kinks which are expected to form in an intersecting string network. Furthermore, once energy is transferred via intersection events from long strings to small loops, these are assumed to decay into gravitational radiation and are removed from the simulation since the gravitational waves are not included in any simulation for obvious reasons of complexity connected to backreaction on the string network.

An alternative approach consists in using simulations of the NG or AH type and the *Unconnected Segment Model* (USM) [25]. The USM model represents the string network as a stochastic ensemble of unconnected moving segments, of length $Ad_{PH}(t)$ and rms velocity v, which are randomly removed at an appropriate rate so as to find sub-horizon decay and the proper string scaling density. The USM model with parameters measured in simulations has been used in the context of CMB anisotropies to reproduce the string power spectra coming from different simulation techniques and derive upper bounds on the string tension parameter. This approach also includes the radiation-matter transition and allows, in principle, to study the effects of deviations from scaling at the onset of a Λ-dominated phase.

As regards the effects on CMB of the network evolution during radiation-matter transition, which sets un upper bound to the applicability of eq. (12) at redshifts presumably even well below $z_{LSS} = 1100$, until about $z \sim 100$, it has been shown [42] that the large-scale anisotropies are primarily produced at $z \lesssim 100$. Since the coherence length of the string network grows with time, anisotropies on small angular scales are expected to be seeded at early times, and the large angle

Table 1 Cosmic string parameters (where v_r and v_m are respectively the *rms* velocities in the radiation- and matter-dominated era) from high resolution simulations performed from '90s to date. The results obtained by Battye-Moss (BM) refer to both USM modeling NG and AH strings. All the other results but those obtained by Bevis and coauthors (BHKU) refer to NG simulations.

Model par	BB [20]	AS [6, 21, 42]	MS [22]	RSB [23]	BHKU (AH) [41]	BM (NG/AH) [25]	BPOS [26]	Δz
$\frac{G\mu}{c^2}$	4×10^{-6}	1.5×10^{-6}		7×10^{-7}	1.8×10^{-6}	$(2.6/6.4) \times 10^{-7}$		
v_r	$0.66c$	$0.62c$	$0.63c$		$0.5c$	$0.65c$ / $0.4c$	$0.63c$	
v_m	$0.61c$	$0.58c$	$0.57c$		$0.5c$	$0.60c$ / $0.4c$	$0.59c$	
A_r	0.14	0.13	0.13	0.16	0.26	0.13/0.35	0.15	
A_m	0.18	0.17	0.20	0.19	0.29	0.21/0.35	0.17	
$N(z)$	$5 - 320$	$6 - 380$	$4 - 230$	$4 - 270$	$1 - 76$	$3 - 200/1 - 43$	$6 - 380$	$(0.5, 7]$
$N(z)$	$360 - 1000$	$420 - 1200$	$260 - 740$	$300 - 860$	$85 - 240$	$220 - 640/48 - 140$	$420 - 1200$	$[8, 100]$
$N(z)$	(1300,2800)	(1500,3400)	(950,3400)	(1100,1800)	(310,430)	(820,3400)/180	(1500,2200)	1100

anisotropies to be seeded at late times. Thus, the contribution of cosmic strings in the redshift range $100 < z < 1100$ should only slightly affect the large angle CMB anisotropy so that the range of interest (11) in this case can be restricted to $z_0 < z \lesssim 100$. At small angular scales the relevant contribution to temperature anisotropy induced by cosmic strings comes from the last scattering epoch where one may expect the strings' signature in the CMB temperature fluctuations to be dominated by the *integrated Sachs-Wolfe* effect from the last scattering surface. It has been shown that at high multipoles the mean angular power spectrum of string-induced CMB temperature anisotropies can be described by a power law slowly decaying as ℓ^{-p}, with $p = 0.889^{+0.001}_{-0.090}$ [43]. This implies that the power spectrum at small angular scales decays much slower than the exponential Silk diffusion damping of the CMB primordial anisotropies. Consequently, the cosmic string contribution to the angular power spectrum can be subdominant at low ℓ while it dominates the primary anisotropies for large values of ℓ. The exponential suppression of the inflationary contribution at high ℓ also means that the string component may dominate for a realistic contribution (i. e. with normalization such that string contribution f_{10} at multipole $\ell = 10$ is 10% of the observed power at this multipole) at $\ell \gtrsim 3500$. The fraction of the total theoretical spectrum due to strings f_ℓ is found to increase [41] from $f_{1500} \approx 0.1$ to $f_{3500} = 0.5$, which points out that a non negligible cosmic strings contribution to the CMB anisotropies is to be searched at small angular scales, corresponding to $\ell \gtrsim 2000$, as soon as they will be accessible. Even though these are the same angular scales for which the *Sunyaev-Zel'dovich* effect begins to make a significant contribution to the temperature power spectrum, this occurs at two observational frequency bands, namely, 100 and 150 GHz, whereas the string contribution is at frequencies in observational bands near 220 GHz, where the Sunyaev-Zel'dovich effect is suppressed.

Although, as already mentioned, the relaxation time for the cosmic string loops to reach a self-similar evolution with respect to the horizon size appears to be larger for smaller loops, the considerable change in scale factor between the GUT redshift and the last scattering surface might well lead the observable length scales

Table 2 The approximate number of string segments for different values of the equation-of-state parameter.

Model par	BB [20]	AS [6, 21, 42]	MS [22]	RSB [23]	BHKU (AH) [41]	BM (NG/AH) [25]	BPOS [26]	Δz
$\frac{G\mu}{c^2}$	4×10^{-6}	1.5×10^{-6}		7×10^{-7}	1.8×10^{-6}	$(2.6/6.4) \times 10^{-7}$		
v_r	$0.66c$	$0.62c$	$0.63c$		$0.5c$	$0.65c \ / \ 0.4c$	$0.63c$	
v_m	$0.61c$	$0.58c$	$0.57c$		$0.5c$	$0.60c \ / \ 0.4c$	$0.59c$	
A_r	0.14	0.13	0.13	0.16	0.26	0.13/0.35	0.15	
A_m	0.18	0.17	0.20	0.19	0.29	0.21/0.35	0.17	
w = − 1.5 $N(z)$	$4 - 330$	$4 - 390$	$3 - 240$	$3 - 280$	$1 - 78$	$3 - 210/1 - 45$	$4 - 390$	$(0.5, 7]$
w = − 1 $N(z)$	$3 - 310$	$4 - 360$	$3 - 220$	$3 - 260$	$1 - 73$	$2 - 190/1 - 42$	$4 - 360$	$(0.5, 7]$
w = − 0.5 $N(z)$	$3 - 270$	$4 - 310$	$3 - 190$	$3 - 230$	$1 - 64$	$2 - 170/1 - 36$	$4 - 310$	$(0.5, 7]$
w = −1.5 $N(z)$	$360 - 980$	$430 - 1200$	$260 - 710$	$310 - 830$	$86 - 230$	$230 - 620/49 - 130$	$430 - 1200$	$[8, 100]$
w = −1 $N(z)$	$340 - 960$	$400 - 1100$	$250 - 700$	$290 - 820$	$83 - 230$	$220 - 610/47 - 130$	$400 - 1100$	$[8, 100]$
w = −0.5 $N(z)$	$300 - 930$	$350 - 1100$	$220 - 680$	$250 - 790$	$72 - 220$	$190 - 590/41 - 130$	$350 - 1100$	$[8, 100]$

of the infinite component of the network to be in scaling at decoupling, $z = 1089$. Such scaling long strings may contribute to the CMB anisotropies down to fairly small angles. On the other hand, including the non-scaling loops, numerical simulations show some extra power at very small scales, which suggests that non-scaling structures start to have significant effects at very small scales, for $\ell \overset{<}{\sim} 10^4$. As regards the relevant contribution due to the infinite component to the CMB anisotropies at moderately high ℓ, the number of string segments in the corresponding range of redshifts close to z_{LSS}, where the network is not expected to have reached the matter era scaling regime, can be estimated as:

$$\frac{8 \ B^3(z)}{A_m^3} < N(z) < \frac{8 \ B^3(z)}{A_r^3}. \tag{25}$$

Let us now consider the deviation from scaling during the matter-dark energy transition, which sets a lower limit at a redshift $z_0 \approx 0.5$ to the applicability of eq. (12). The number of cosmic string segments at $z \overset{<}{\sim} 1$ could be extremely small so that it would become important to understand how deviation from the scaling behavior around the present cosmological era may affect the network since an eventual network no longer scaling with matter, exponentially slowed down, could be quite difficult to detect. As previously mentioned, the string velocity plays an important role for detecting signatures in the CMB since it determines the amplitude of the line-like discontinuities in the CMB temperature. As for the gravitational lensing there is no such restriction to relativistic velocities for observation to succeed but the number of string segments in the range of optical sources could be a very small fraction of the initial number and approaching $z \overset{<}{\sim} 1$ it could become a small fraction even of the expected number in the effective observable (visible) universe. This can be seen by averaging on the values presented

in Table 1 and taking into account that at $z = 1100$ because of the deviation from scaling $N^{av}(z)$ is expected to be less than the actual number. Thus, assuming that the most distant object we are able to observe by optical methods are located at a redshift $z = 7$, the probability to observe strings crossing the effective observable universe in the optical range is proportional to the volume of the optical sphere, having radius $d(z = 7) = B(z = 7)d_{PH}$. In horizon units then $p \sim B^3(7) = 0.24$ ($B(7) = 0.62$) and the corresponding angular size of a string eventually observed is $\sim 100^o$ [27]. For smaller values of the redshift the number of string segments inside the sphere becomes increasingly smaller and the angular size larger. For instance, at a redshift $z = 2$ the probability is reduced to $p \sim B^3(2) = 0.05$ ($B(2) = 0.37$) and the angular size of the string is around $\sim 134^o$. Below $z \lesssim 1$ the number of string segments inside the sphere of radius $d(z \lesssim 1)$ is expected to be so small (see Table 1) as to render detection by optical methods in this range a challenging problem unless the deviation from scaling at transition to the dark energy era is such that the decrease in reconnection events, whose effect is to increase the density of strings and the time needed to reach equilibrium, may somewhat compensate the eventual dilution by exponential expansion maintaining the number of strings to a detectable level.

As regards the dark energy variants of the standard cosmology, a different choice of the equation-of-state parameter implies increasing or decreasing distances and hence volumes defined through such distances. These volume effects are due to a different expansion rate: phantom models have always a larger volume than the ΛCDM model since the expansion rate is larger, while quintessence models have a smaller volume than the ΛCDM model being the expansion rate lower. As a consequence, one can only find an increased or decreased number of string segments, being the characteristic length scale of the network unaltered. The number of string segments for $w \in \{-1.5, -1, -0.5\}$ is presented in Table 2. As we can see from Figure 1, $B(z)$ is slightly dependent of w and a comparison of the results obtained in the two ranges of z (Table 2) points out that at very small redshifts it makes no substantial difference whether we use the ΛCDM or some other CDM model. Therefore for the considerations that follow, which apply to small values of redshift, for definiteness, we refer to the ΛCDM cosmology, but they can be easily extended to the above mentioned variants.

Taking into account both the constraints on the string tension parameter set by gravitational lensing ($G\mu/c^2 < 3 \times 10^{-7}$) and by CMB power spectrum which, considering the BM result for NG strings $G\mu/c^2 < 2.6 \times 10^{-7}$ and the stricter constraint coming from the Atacama Cosmology Telescope (ACT) [44], $G\mu/c^2 < 1.6 \times 10^{-7}$, may be suitably chosen in the middle of this range, we can get some further insight on the probability of observing cosmic strings through gravitational lensing events for static straight strings. Since the angular separation between the lensed images,

$$\delta\phi = \Delta \frac{D_{ls}}{D_{os}} sin\theta \qquad \theta \in [0, \pi]\,, \tag{26}$$

depends on Δ as well as on the ratio between the angular diameter distances from source to string (lens), D_{ls}, and from source to observer, D_{os}, and on the angle θ between the string direction and the line of sight, not all the strings contained in the sphere of the optical sources can be observed through their gravitational lensing effects. For a straight string segment lying at z close to the upper limit

of the optical range the corresponding lensing angle would be on the border of observability ($< 0.07''$), being $D_{ls} \ll D_{os}$, even in the ideal case $sin\theta = 1$, although $N(z)$ is still quite large (on average about 270). For the most distant sources at $z \sim 6 - 7$ therefore the string-lens is required to be at $z \lesssim 5$ in order to yield observable effects. For non ideal strings an additional factor less than unity for $\theta \neq \pi/2$ restricts the strings that have more probability to be observed to those located at redshifts around $z \lesssim 2$ (where the average number of string segments is expected to be < 60), which implies a cut on the highest values of z in the optical sources range at redshifts where the expected number of string segments is quite large. Setting a lower bound to the possible redshifts where one can reasonably suppose to find more than one string across the visible universe at the redshift of the transition matter-dark energy results in a further reduction of the probability of observing gravitational lensing events for the most distant and rare sources.

If we consider that the most part of the observed quasars and galaxies are distributed at redshifts $1 \lesssim z \lesssim 2$, the range of redshifts at which the probability of observing cosmic strings by their gravitational lensing effects is greatest will be $0.6 \leq z < 1$ (where N(z) is on average < 15). For a source at $z_s \in [1, 2]$ and a segment of string at a redshift $z_l \in [0.6, 1)$ the corresponding lensing angle is in principle always sufficiently large for ideal strings to produce two distinguishable images of the source when this one is a quasar. As regards galaxies, only the points interior to the strip defined by the deficit angle will appear duplicated the other side of the string. The outer points will be cut away resulting in visible sharp edges in the isophotes of the source images [45]. In the case of non ideal strings even for strings close to the lower limit of the matter dominated era the corresponding lensing angle can be too small to be observable for some values of θ. Let us consider, for instance, randomly oriented static strings located at redshifts $0.6 \leq z_l < 1$ which could be gravitational lenses for any sources in the above mentioned redshifts range. Outside of a certain interval of values of θ, $\delta\phi$ becomes smaller than the angular resolution even of space-based telescopes ($0.05''$ to $0.1''$). Since this interval is almost different for any value of z_l, in order to have an idea of the number of observable strings for any value of the range of $z_l \in [0.6, 1)$ and for any value of the source redshift $z_s \in [1, 2]$ we have to calculate the probability of observing a cosmic string in a given volume which form with the line of sight an angle θ contained in the corresponding interval for each interval separately. By adding the results we find that the total amount of segments of static straight string which can produce observable gravitational lensing effects for any sources located at $z_s \in [1, 2]$ is reduced of about a half with respect to the case of ideal strings. For $1 \leq z_l < 2$, as z_l increases, the ratio between the angular distances decreases so that even small deviations from the ideal case can yield undetectable lensing angles. $\delta\phi$ is no longer detectable for $z_l \sim 1.8$ even for ideal cosmic strings. Of all the strings contained in the spherical shell determined by $z_l \in [1, 2)$ only a small fraction (about one over four) may have a $\delta\phi$ potentially observable for sources located at $z_s \in (1, 2]$.

An exhaustive treatment on the topic involving survey fields, distribution of sources at different redshifts and their brightness and the string velocity is beyond the scope of this paper.

The outcome of the above reasoning focused on the most favorable case of the redshifts range of sources where the observed objects are more numerous and brighter is of course also a consequence of the small value chosen for Δ. Thus, if

we apply the same considerations to cosmic superstrings we will have significant differences due to the fact that, while the D and FD components of the network have tensions comparable to those of ordinary cosmic strings, the F component is expected to have smaller tension, $G\mu_F/c^2 \sim 10^{-8}$, for a small value of the string coupling constant ($g_s \sim 10^{-2}$). This leads to excessively small values of the lensing angle, $\delta\phi \leq 0.05''$, even in the ideal case of string segments perpendicular to the line of sight. As a consequence, although a small value of the string coupling constant yields an exceedingly large number of string segments ($\sim 10^3$) for the F component even at small redshifts (down to the value $z_l \sim 0.6$) against the small number found for ordinary cosmic strings, models supporting a small value of the string coupling constant cannot be ruled out on the grounds of the predicted large number of the F component as long as the range of small values of tension involved are still unexplored by means of current technology. The case of cosmic superstrings will be discussed in detail in a forthcoming paper. Here we merely point out that a small value of $\Delta \sim 0.09''$ also leads to temperature jumps in the CMB radiation (KS effect) no longer appreciable so that the presence of a large number of F strings does not conflict with observations.

References

1. T.W.B. Kibble,*Topology of Cosmic Domains and Strings*, J. Phys. A9, 1387, 1976.
2. A. Vilenkin, E.P.S. Shellard, *Cosmic Strings and other Topological Defects*, Cambridge University Press, 1995.
3. R. Durrer, *Topological Defects in Cosmology*, New Astron. Rev.43 111, 1999.
4. J. Magueijo, R.H. Brandenberger, *Cosmic Defects and Cosmology*, arXiv:astro-ph/0002030, 2000.
5. T. Vachaspati, *Lectures on Cosmic Topological Defects*, arXiv: hep-ph/0101270, 2001.
6. E.P.S. Shellard, B. Allen, *On the Evolution of Cosmic String*, in *Formation and Evolution of Cosmic Strings*, G.W. Gibbons, S.W. Hawking, T. Vachaspati, Cambridge University Press, 1990.
7. M.B. Hindmarsh, T.W.B. Kibble, *Cosmic Strings*, Rept. Prog. Phys. 58, 477, arXiv:hep-ph/9411342, 1994.
8. M. Hindmarsh, S. Stuckey, N. Bevis, *Abelian Higgs Cosmic Strings: Small Scale Structure and Loops*, Phys. Rev. D79, 123504, arXiv:0812.1929 [hep-th], 2008.
9. S. Kachru, R. Kallosh, A. Linde, J. Maldacena, L. McAllister, S.P. Trivedi, *Towards Inflation in String Theory*, JCAP 0310, 013, arXiv:hep-th/0308055, 2003.
10. N. Arkani-Hamed, S. Dimopoulos, G. Dvali, *The Hierarchy Problem and New Dimensions at a Millimeter*, Phys. Lett. B429, 263, arXiv:hep-ph/9803315, 1998.
11. I. Antoniadis, N. Arkani-Hamed, S. Dimopoulos, G. Dvali, *New Dimensions at a Millimeter to a Fermi and Superstrings at a TeV*, Phys. Lett. B436, 257, arXiv:hep-ph/9804398, 1998.
12. E.J. Copeland, R.C. Myers, J. Polchinski, *Cosmic F- and D-strings*, JHEP 0406, 013, arXiv:hep-th/0312067, 2004.
13. N. Jones, H. Stoica, S.H. Henry Tye, *The Production, Spectrum and Evolution of Cosmic Strings in Brane Inflation*, Phys. Lett. B 563, 6, arXiv:hep-th/0303269, 2003.
14. N. Kaiser, A. Stebbins, *Microwave Anisotropy due to Cosmic Strings*, Nature 310, 391, 1984.
15. M.G. Jackson, N.T. Jones, J. Polchinski, *Collisions of Cosmic F- and D-String*, JHEP 0510, 013, arXiv:hep-th/0405229, 2005.

16. A. Avgoustidis, E.P.S. Shellard, *Effect of Reconnection Probability on Cosmic (Super)string Network Density*, Phys. Rev. D73, 041301, arXiv:astro-ph/0512582, 2005.
17. S.H. Henry Tye, I. Wasserman, M. Wyman, *Scaling of Multi-Tension Cosmic Superstring Networks*, Phys. Rev. D 71, 103508 [Erratum: ibid. 71, 129906], arXiv:astro-ph/0503506, 2005.
18. A. Pourtsidou, A. Avgoustidis, E.J. Copeland, L. Pogosian, D.A. Steer, *Scaling Configurations of Cosmic Superstring Networks and their Cosmological Implications*, Phys. Rev. D83, 063525, arXiv:1012.5014 [astro-ph.CO], 2011.
19. A. Achucarro, R. de Putter, *Effective Non-Intercommutation of Local Cosmic Strings at High Collision Speeds*, Phys. Rev. D74, 121701, arXiv:hep-th/0605084, 2006.
20. D.P. Bennett, F.R. Bouchet, *High Resolution Simulations of Cosmic String Evolution I: Network Evolution*, Phys. Rev. D41, 2408, 1990.
21. B. Allen, E.P.S. Shellard, *Cosmic String Evolution: A Numerical Simulation*, Phys. Rev. Lett. 64, 119, 1990.
22. C.J.A.P. Martins, E.P.S. Shellard, *Fractal Properties and Small-scale Structure of Cosmic String Networks*, Phys. Rev. D73, 043515, arXiv:astro-ph/0511792, 2005.
23. C. Ringeval, M. Sakellariadou, F.R. Bouchet, *Cosmological Evolution of Cosmic String Loops*, JCAP 0702, 023, arXiv:astro-ph/0511646, 2007.
24. N. Bevis, M. Hindmarsh, M. Kunz, J. Urrestilla, *CMB Polarization Power Spectra Contributions from a Network of Cosmic Strings*, Phys. Rev. D76, 043005, arXiv:0704.3800 [astro-ph], 2007.
25. R. Battye, A. Moss, *Updated Constraints on the Cosmic String Tension*, Phys. Rev. D82, 023521, arXiv:1005.0479 [astro-ph.CO], 2010.
26. J.J. Blanco-Pillado, K.D. Olum, B. Shlaer, *Large Parallel Cosmic String Simulations: New Results on Loop Production*, arXiv:1101.5173v2 [astro-ph.CO], 2011.
27. O.S. Sazhina, M.V. Sazhin, V.N. Sementsov, *Cosmic Microwave Background Anisotropy Induced by a Moving Straight Cosmic String*, Journal of Experimental and Theoretical Physics 106, 878;
28. O.S. Sazhina, M.V. Sazhin, V.N. Sementsov, M. Capaccioli, G. Longo, G. Riccio, G. D'Angelo, *CMB Anisotropy Induced by a Moving Straight Cosmic String*, arXiv:0809.0992 [astro-ph], 2008.
29. M.V. Sazhin, O.S. Sazhina, M. Capaccioli, G. Longo, M. Paolillo, G. Riccio, *Gravitational Lens Images Generated by Cosmic Strings*, The Open Astronomy Journal, 3, 200, 2010.
30. http://lambda.gsfc.nasa.gov/product/map/dr4/best_params.cfm.
31. D.J. Eisenstein, *Detection of the Baryon Acoustic Peak in the Large-Scale Correlation Function of SDSS Luminous Red Galaxies*, Astrophys. J. 633, 560, arXiv:astro-ph/0501171, 2005.
32. D.S. Gorbunov, V.A. Rubakov, *Vvedenie v teoriyu rannei Vselennoy - Introduction to Modern Cosmology*, URSS, Moscow, 2008.
33. R.R. Caldwell, *A Phantom Menace?*, Phys. Lett. B 545, 23, arXiv:astro-ph/9908168, 2002.
34. J. Frieman, M. Turner, D. Huterer, *Dark Energy and the Accelerating Universe*, arXiv:0803.0982 [astro-ph], 2008.
35. E.J. Copeland, M. Sami, S. Tsujikawa, *Dynamics of Dark Energy*, Int. J. Mod. Phys. D 15, 1753, [arXiv:hep-th/0603057], 2006.
36. M.V. Sazhin, O.S. Sazhina, U. Chadayammuri, *The Scale Factor in the Universe with Dark Energy*, arXiv:1109.2258 [astro-ph.CO], 2011.
37. A.G. Riess et al., *Type Ia Supernova Discoveries at z > 1 from the Hubble Space Telescope: Evidence for Past Deceleration and Constraints on Dark Energy Evolution*, Astrophys. J. 607, 665, arXiv:astro-ph/0402512, 2004.
38. Y.L. Bolotin, O.A. Lemets, D.A. Yerokhin, *Expanding Universe: Slowdown or Speedup?*, arXiv:1108.0203 [astro-ph.CO], 2011.
39. A. Albrecht, R.A. Battye, J. Robinson, *A Detailed Study of Defect Models for Cosmic Structure Formation*, Phys. Rev. D59, 023508, arXiv:astro-ph/9711121, 1997.
40. R.A. Battye, J. Robinson, A. Albrecht, *Structure Formation by Cosmic Strings with a Cosmological Constant*, Phys. Rev. Lett. 80, 4847, arXiv:astro-ph/9711336, 1998.
41. N. Bevis, M. Hindmarsh, M. Kunz, J. Urrestilla, *CMB Power Spectra from Cosmic Strings: Predictions for the Planck Satellite and beyond*, Phys. Rev. D82, 065004, arXiv:1005.2663 [astro-ph.CO], 2010.
42. B. Allen, R.R. Caldwell, E.P.S. Shellard, A. Stebbins, S. Veeraraghavan, *Large Angular Scale CMB Anisotropy Induced by Cosmic Strings*, Phys. Rev. Lett. 77, 3061, arXiv:astro-ph/9609038, 1996.

43. A.A. Fraisse, C. Ringeval, D.N. Spergel, F.R. Bouchet, *Small-Angle CMB Temperature Anisotropies Induced by Cosmic Strings*, Phys. Rev. D78, 043535, arXiv:0708.1162 [astro-ph], 2008.
44. J. Dunkley et al., *The Atacama Cosmology Telescope: Cosmological Parameters from the 2008 Power Spectra* Astrophys. J. 739, 52, arXiv:1009.0866 [astro-ph.CO], 2011.
45. M.V. Sazhin, O.S. Khovanskaya, M. Capaccioli, G. Longo, M. Paolillo, G.Covone, N.A. Grogin, E.J. Schreier, *Gravitational Lensing by Cosmic Strings: What We Learn from the CSL-1 Case*, Mon. Not. Roy. Astron. Soc. 376,1731, arXiv:astro-ph/0611744, 2007.